Microchemical Journal 145 (2019) 864–871

Contents lists available at ScienceDirect

Microchemical Journal

journal homepage: www.elsevier.com/locate/microc

A visualized colorimetric detection strategy for heparin in serum using a metal-free polymer nanozyme

Mengyuan Yin[a], Zhiqiang Duan[a,b,*], Chunxian Zhang[a], Luping Feng[a], Yuqi Wan[a], Yuanyuan Cai[a], Huan Liu[a], Shuai Li[a], Hua Wang[a,b,*]

[a] Institute of Medicine and Materials Applied Technologies, College of Chemistry and Chemical Engineering, Qufu Normal University, Qufu, Shandong 273165, PR China
[b] Shandong Sunshine New Materials Science and Technology Co., LtD., Jining City, Shandong Province, PR China

ARTICLE INFO

Keywords:
Metal-free polymer nanozyme
Peroxidase-like activity
Chromogenic reaction
Electrostatic attraction
Heparin

ABSTRACT

A metal-free polymer nanozyme has been developed for the first time simply via the one-pot covalent reaction of hyperbranched polyethyleneimine (PEI) and redox dihydroxybenzaldehyde (DHB). The yielded PEI-DHB nanoparticles could display the peroxidase-like catalysis activity, so as to act as the metal-free nanozyme in catalyzing the chromogenic reactions of 3,3′,5,5′-tetramethylbenzidine and H_2O_2. More interestingly, the catalysis activity of the polymer nanozymes could be specifically inhibited by heparin oppositely charged. A facile visualized colorimetric method was thereby developed for sensing heparin through combining the specific catalysis and electrostatic attraction of PEI-DHB nanozyme. It was found that the developed colorimetric method can enable the detection of heparin in serum over the linear concentration range of 0.050–1.0 μM, promising the wide applications for the detection of heparin in the clinical laboratory for the disease diagnostics and pharmacological monitoring. More importantly, such a green synthesis method may be tailored for fabricating various metal-free polymer nanozymes for the wide catalysis applications.

1. Introduction

Over the past few years, nanomaterial-based enzyme mimics (nanozymes) have received remarkable attentions in the applications for designing different sensing platforms [1–2]. Compared with natural enzymes, these nanozymes can exhibit some excellent advantages such as high surface-to-volume ratios, easy preparation, and high stability against harsh environmental conditions. Since the first discovery that Fe_3O_4 nanoparticles (NPs), which were usually applied for magnetic separation [3], can possess intrinsic enzymatic activity [4], various metal-based inorganic nanomaterials such as metal oxide NPs and noble metal NPs have been reported as artificial enzymes or electrocatalysis materials [5–12]. Despite great advances have been obtained, these metal-based nanozymes may suffer from some disadvantages such as metal toxicity and spontaneous aggregations in aqueous solutions, which may hamper their wide catalysis applications. Alternatively, some metal-free nanozymes have been recently explored with low toxicity and high biocompatibility, most known as carbon nanocomposites [13–15]. For example, Huang and co-workers reported carbon nanodots possess the peroxidase-like activity for catalyzing the chromogenic reactions with a detectable color change [13]. Li's group described the application of graphene dots with peroxidase-like catalysis for the detection of glucose and glutathione [14]. Single-walled carbon nanohorns have also be employed as nanozymes for the glucose determination in serum [15]. Nevertheless, these metal-free inorganic nanozymes may be trapped by either harsh preparation process or moderate catalysis activities. Recent years have witnessed the rapid development of nanozymes made from some functional polymers showing several important advantages like low toxicity, easy modification, simple preparation, good dispersion or solubility, favorable aqueous stability, and environmentally benign materials [17,18]. For this case, the catalysis performances of these nanozymes can largely depend on the polymers used. As an environmentally benign polymer representative, hyperbranched polyethyleneimine (PEI) features some outstanding merits such as good water solubility, ease usage, and biological affinity [19]. Particularly, nanozymes made from PEI can expect the pretty high density of positive charges, thus making it a suitable candidate for strongly interacting with some negatively charged targets such as heparin [20]. To the best of our knowledge, however, the application of PEI for the design of metal-free nanozymes has hardly been

* Corresponding authors at: Institute of Medicine and Materials Applied Technologies, College of Chemistry and Chemical Engineering, Qufu Normal University, Qufu, Shandong 273165, PR China.
E-mail addresses: duan198402@126.com (Z. Duan), huawang@qfnu.edu.cn (H. Wang).
URLs: http://wang.qfnu.edu.cn (Z. Duan), http://wang.qfnu.edu.cn (H. Wang).

https://doi.org/10.1016/j.microc.2018.11.059
Received 14 October 2018; Received in revised form 3 November 2018; Accepted 30 November 2018
Available online 03 December 2018
0026-265X/

explored to date.

Heparin, a negatively charged polysaccharide in biological systems, plays a significant role in various physiological processes [21]. Especially, it may act as a vital anticoagulant drug to prevent thrombosis during cardiovascular surgery or to treat thrombotic diseases [22,23]. Nevertheless, abnormal heparin dose in human body could induce some serious complications such as hemorrhage and thrombocytopenia [24]. Over the past decades, a variety of conventional detection methods have been developed for the analysis of heparin, most known as the anion exchange chromatography, nuclear magnetic resonance, capillary electrophoresis, potentiometric test, fluorescent analysis, and colorimetric detection methods [25–33]. Among these classic detection methodologies, colorimetric analysis methods with the simplicity, sensitivity, and visual detection properties have attracted increasing attentions [34]. Particularly, a diverse of colorimetric methods have been reported for the detection of heparin [35–38], however, some drawbacks like complicated operation, bulky instruments, and moderate sensitivity may limit their large-scale applications in the clinical diagnostics practice. Therefore, exploring a rapid, simple, sensitive, and field-applicable colorimetric analysis method for the determination of heparin is still of great interest in the clinical disease diagnostics and pharmacological monitoring fields.

In the present work, a metal-free polymer nanoparticles with peroxidase-like activity has been developed for the first time by covalently coupling hyperbranched PEI with redox dihydroxybenzaldehyde (DHB) yielding the PEI-DHB NPs, with the fabrication principle and procedure schematically illustrated in Scheme 1. Herein, the facile one-pot synthesis of PEI-DHB NPs was conducted via the catalyst-free Schiff base reaction at room temperature (Scheme 1A), in contrast to the most metal-free nanozymes reported elsewhere prepared by multiple steps and/or at high temperature [13–15]. It was discovered that the so yielded PEI-DHB NPs could display the good aqueous dispersion, storage stability, and well-defined morphological structures. Importantly, they could display the strong peroxidase-like catalysis activity for catalyzing the chromogenic reactions of 3,3′,5,5′-tetramethylbenzidine (TMB)-H_2O_2 substrate to generate color change. Herein, DHB with the phenolic hydroxy groups on benzene rings should serve as the catalysis-active sites for catalyzing the chromogenic reactions [39]. Moreover, heparin would readily access to the oppositely-charged PEI-DHB NPs to act as the capping agents to densely block the catalysis-active sites of the developed metal-free nanozymes resulting in the greatly inhibited catalysis activity toward a colorimetric detection strategy for probing heparin in serum.

2. Experimental section

2.1. Materials and instruments

Heparin (sodium salt; MW 17,000-19,000) from porcine intestinal mucosa, hyperbranched polyethyleneimine (PEI), 3,4-dihydroxybenzaldehyde (DHB), chondroitin sulphate sodium salt (Chs) from shark cartilage, hyaluronic acid (HA) (sodium salt) from bovine vitreous humor, nicotinic acid (NA),bovine serum albumin (BSA), amino acids, urea, uric acid (UA), fructose (Fru), sucrose (Suc), glucose (Glu),

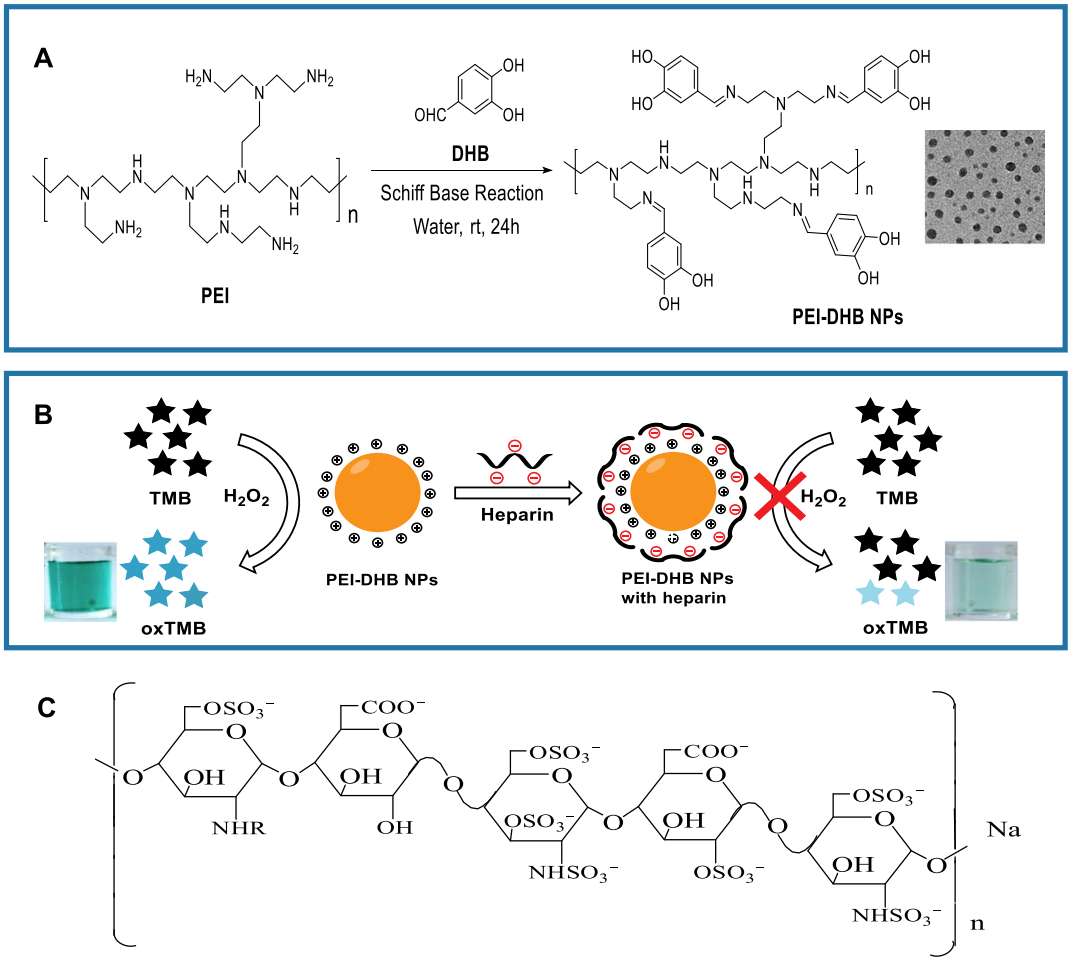

Scheme 1. Schematic illustration of (A) the main principle and procedure for the synthesis of PEI-DHB NPs by the Schiff base reaction with the TEM image; (B) the peroxidase-like catalysis activity of PEI-DHB NPs in catalyzing the TMB-H_2O_2 reactions that can be specifically inhibited by heparin with (C) molecular structure.

metal ions, and 3,3′,5,5′-tetramethylbenzidine (TMB), were obtained from Sigma-Aldrich. All other reagents were analytical grade. Sterile water from deionized water (> 18 MΩ, RNase-free) was supplied from an Ultra-pure water system (Pall, USA) for high pressure sterilizer.

UV–vis spectrophotometer (Shimadzu, UV-3600, Japan) and Transmission electron microscopy (TEM, JEOL, Ltd., Japan) were separately applied for the characterization of different materials or products. Fourier transform infrared (FTIR) spectra were obtained by FTIR spectrophotometer (Thermo Nicolet Nexus 470FT, USA).

2.2. Synthesis of metal-free polymer nanozyme

An aliquot of PEI (5.0 mg mL^{-1}) and DHB (2.0 μM) were mixed in water of 50.0 mL. Then the mixture was stirred at room temperature for 24 h. Subsequently, the as-prepared PEI-DHB NPs solution was dialyzed against ultrapure water through a dialysis membrane (molecular weight cut off 1000 Da) for 48 h. The product inside the dialysis bag was collected for further experiments.

2.3. Peroxidase-like catalysis activity of PEI-DHB NPs

The as synthesized PEI-DHB NPs (30.0 μL, 5.0 mg mL^{-1}) were introduced into the buffer solution (100.0 mM, pH 2.0–12.0) containing TMB (2.0 mM), H_2O_2 (20.0 mM) for 20 min at 37 °C. The absorption spectra of the resulting products were recorded using a UV–vis spectrophotometer. The optimization of the PEI-DHB NPs peroxidase-like activity was conducted separately using different amounts of PEI-DHB NPs, pH values, temperature, and H_2O_2 concentrations. The reaction kinetic measurements were carried out in time course mode by monitoring the absorbance changes at 652 nm. Experiments were conducted using PEI-DHB NPs (150.0 μg mL^{-1}) in buffer (pH 3.0) containing 2.0 mM TMB or 20.0 mM H_2O_2. Steady-state reaction rates at different concentrations of substrate were obtained by calculating the time-dependent slopes of initial absorbance. The Michaelis-Menten constant was calculated using the Lineweaver-Burk plot: $1/\nu = (K_m / V_{max})(1 / [S] + 1 / K_m)$, where ν is the initial velocity, K_m is the Michaelis constant, V_{max} is the maximal reaction velocity, and [S] is the concentration of substrate.

2.4. Colorimetric detection of heparin

The selective colorimetric analysis was performed for heparin, taking the possibly interferential substances commonly existing in serum as the control tests, including Chs, HA, NA, BSA, Homocysteine (Hcy), L-glycine (Gly), L-phenylalanine (Phe), L-cysteine (Cys), L-arginine (Arg), L-Valine (Val), L-lysine (Lys), L-Alanine (Ala), L-Leucine (Leu), urea, UA, Fru, Suc, Glu, Na^+, K^+, Fe^{2+}, Fe^{3+}, Co^{2+}, Ca^{2+}, Mg^{2+}, Zn^{2+}, Cl^-, CO_3^{2-}, and PO_4^{3-}. Heparin detection was performed as follows: PEI-DHB NPs (150.0 μg mL^{-1}) were directly incubated with various concentrations of heparin in HAc-NaAc buffer solution (0.20 M, pH 3.0) for 10 min at ambient temperature. After 10 min incubation at ambient temperature, a mixture of TMB (2.0 mM), H_2O_2 (20.0 mM) was introduced, after the reaction underwent for 20 min, the absorption spectra were collected using a UV–vis spectrophotometer. Relative absorbance is defined as $[(A_0 - A) / A_0]$ (λ_{max} = 652 nm), where A and A_0 refer to the absorbance in the presence and absence of heparin, respectively. In addition, the heparin-spiked samples were obtained according to the following procedure. The blood samples obtained from the patients in a local hospital were first spiked with a determined amount of heparin for anticoagulation, and then centrifuged for 20 min. Furthermore, the so obtained supernatants were collected as the serum samples that were further diluted with the testing buffer (HAc-NaAc, pH 3.0). The yielded serum samples containing various levels of heparin were subsequently applied for the colorimetric determinations.

3. Results and discussion

3.1. Main fabrication principle and sensing procedure of peroxidase-like PEI-DHB NPs for the inhibition-based analysis of heparin

Scheme 1 schematically illustrates the main fabrication principle and sensing procedure of peroxidase-like PEI-DHB NPs for the inhibition-based analysis of heparin. Herein, hyperbranched PEI was covalently bound with redox DHB by the Schiff base reaction to yield PEI-DHB NPs with the morphologically spheric structures as disclosed by the TEM image (Scheme 1A). The resulting metal-free nanozymes could display the strong peroxidase-like catalysis in the oxidization reactions of TMB-H_2O_2 substrate producing a color change (Scheme 1B), in which DHB with redox phenolic hydroxy groups on benzene rings would act as the catalysis-active sites in catalyzing the chromogenic reactions, as described previously for the enzyme-like fluorescein [39]. More importantly, it was discovered that the as-prepared PEI-DHB NPs with positively-charged PEI carriers can strongly interact with negatively-charged heparin [21,40]. Herein, heparin, a negatively-charged polysaccharide polyelectrolyte (Scheme 1C), can display the powerful electrostatic adsorption with the oppositely-charged PEI-DHB polyelectrolyte, which is much stronger than those of other small molecules (i.e., amino acids) or ions tested afterwards. Accordingly, heparin would act as the capping agents to densely block the catalysis-active sites of the developed metal-free nanozymes leading to the dramatic inhibition of their catalysis activity. A visualized colorimetric detection strategy was thereby developed for selectively probing heparin in serum afterwards.

3.2. Characterization of the nanocatalysts of PEI-DHB NPs

UV–vis and FTIR spectroscopy studies were separately conducted

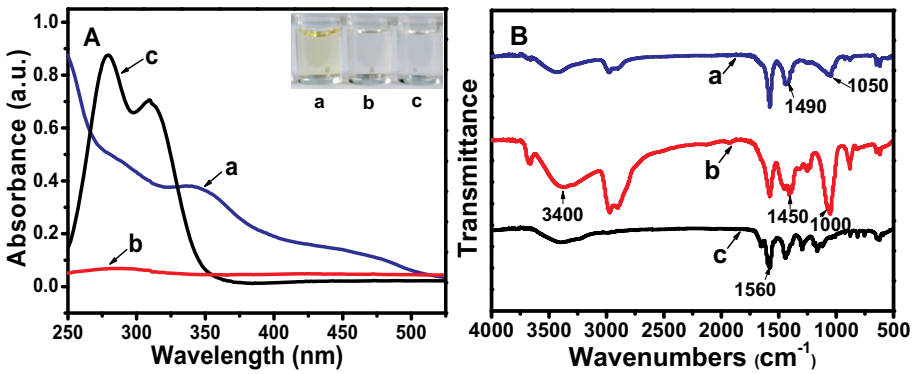

Fig. 1. (A) UV–vis absorption spectra (B) FTIR spectra of (a) PEI-DHB NPs, (b) PEI, and (c) DHB.

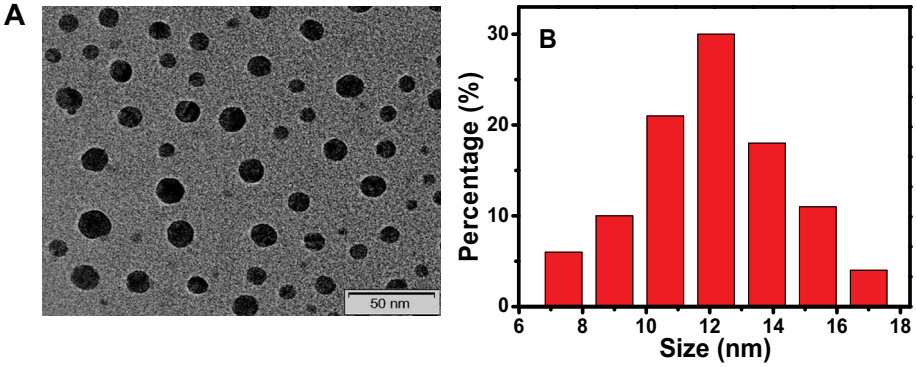

Fig. 2. (A) TEM image (B) the size distribution of the PEI-DHB NPs.

for PEI-DHB NPs, taking native PEI and DHB as the controls (Fig. 1). It was discovered that the PEI-DHB NPs could exhibit the absorption peaks in the range of 330–370 nm (Fig. 1A, curve a), which can be ascribed to n → π* transitions of C=N bonds. Compared to the typical absorption peaks of DHB (Fig. 1A, curve c), the peak at 275 nm and 320 nm disappeared, suggesting the C=N bonds formation in the PEI-DHB NPs. Moreover, Fig. 1B shows the comparison of FTIR spectra among these testing substances. One can find that the spectra of the PEI-DHB NPs (curve a) can include the typical characteristic peaks of native PEI (curve b). Notably, the stretching vibration peak at 1560 cm^{-1} of aldehyde C—H of DHB (curve c) would be absent upon the formation of the PEI-DHB NPs (curve a). In comparison to the aldehyde vibration peak at 1600 cm^{-1} of DHB and -NH_2 groups vibration peak at 3400 cm^{-1} of PEI [44], PEI-DHB NPs displayed separately the weakened ones (curve a), thus confirming the conjugated formation of PEI-DHB NPs. Furthermore, the morphological structure of the as-prepared PEI-DHB NPs was investigated by TEM imaging (Fig. 2). As shown in Fig. 2B, the prepared PEI-DHB NPs could be uniformly dispersed with the spherical profile, showing the average particle size of about 12.5 nm in diameter.

3.3. Peroxidase-like activity of PEI-DHB NPs

Colorimetric investigations were carried out on the peroxidase-like catalysis performances of PEI-DHB NPs using the TMB-H_2O_2 reaction system. It was discovered that PEI-DHB NPs could catalyze the chromogenic TMB-H_2O_2 reaction yielding the blue products with a strong absorbance at 652 nm (Fig. 3A, curve a). Furthermore, the introduction of heparin could apparently inhibit the catalysis of the PEI-DHB NPs in the chromogenic reaction (curve b), showing the greatly decreased absorbance of reactant product. As aforementioned, herein, heparin could serve as the capping agent to encapsulate the oppositely charged PEI-DHB NPs through the electrostatic attraction leading to the decrease in their catalysis activity, so that the specific catalysis inhibition-based colorimetric detection for heparin could thereby be expected. The effects of PEI-to-DHB ratios used on the catalytic activity of PEI-DHB NPs were investigated (Fig. 3B). One can find that the optimum PEI-to-DHB ratios of 10/1 should be selected for the preparation of PEI-DHB NPs. Furthermore, the main catalysis conditions of PEI-DHB nanozymes were explored by catalyzing the chromogenic TMB-H_2O_2 reactions, including PEI-DHB NPs dosages, reaction temperature, pH values, and TMB-H_2O_2 ratios, with the data shown in Fig. 4. Accordingly, the most suitable catalysis conditions for the chromogenic reactions were obtained including 150.0 μg mL^{-1} PEI-DHB NPs and TMB-H_2O_2 ratio of 1/10 at pH 3.0 under 37 °C. Besides, the prepared PEI-DHB NPs could well maintain the high catalysis activity over considerably wide H_2O_2 concentrations (Fig. 4D, insert), indicating that the nanozymes would facilitate the wide catalysis applications under the harsh testing conditions.

To better understand the peroxidase-like catalysis performances of PEI-DHB NPs, steady-state kinetics were studied with the TMB and H_2O_2 substrates (Fig. 5). The data were obtained by varying one substrate concentrations while keeping the other substrate concentration constant. It was found from Fig. 5 that the typical Michaelis-Menten curves were obtained for PEI-DHB NPs at different concentrations of H_2O_2 (Fig. 5A) and TMB (Fig. 5B). Further, the Michaelis-Menten constant (K_m) and the maximum initial velocity (V_{max}) are thus derived by the Lineweaver-Burk plotting separately for TMB (Fig. 5C) and H_2O_2 (Fig. 5D), with the parameters summarized in Table 1 in comparison with those obtained by the artificial enzymes reported previously. By comparison, obviously, PEI-DHB NPs could present a lower or comparable K_m values separately for H_2O_2 and TMB, indicating that the as-synthesized nanozyme could display favorable affinities to the substrates of catalytic reactions. That is, the PEI-DHB NPs can exhibit better or comparable catalysis performances than those of other kinds of metal-free peroxidase mimics.

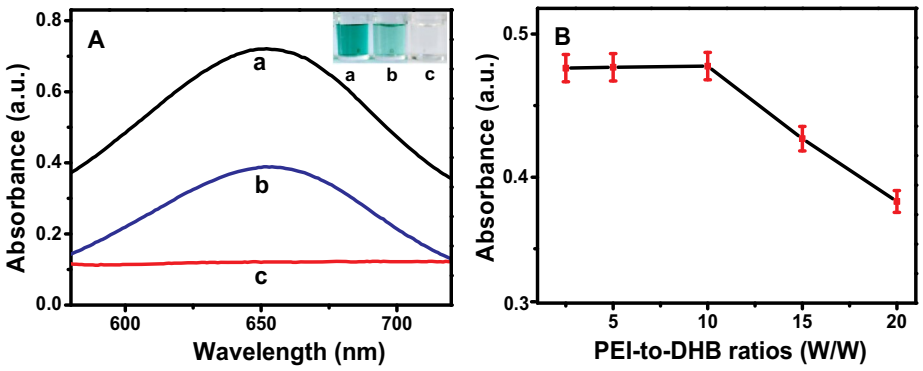

Fig. 3. (A) Typical UV–vis absorption spectra of the products of TMB-H_2O_2 reaction catalyzed by PEI-DHB NPs in the (a) absence and (b) presence of heparin, taking (c) TMB-H_2O_2 as the controls (insert: the photographs of the corresponding reaction solutions), where TMB (2.0 mM), H_2O_2 (20.0 mM), heparin (1.0 μM), and PEI-DHB NPs (150.0 μg mL^{-1}) were used; (B) the effects of PEI-to-DHB ratios on the catalytic activity of PEI-DHB NPs.

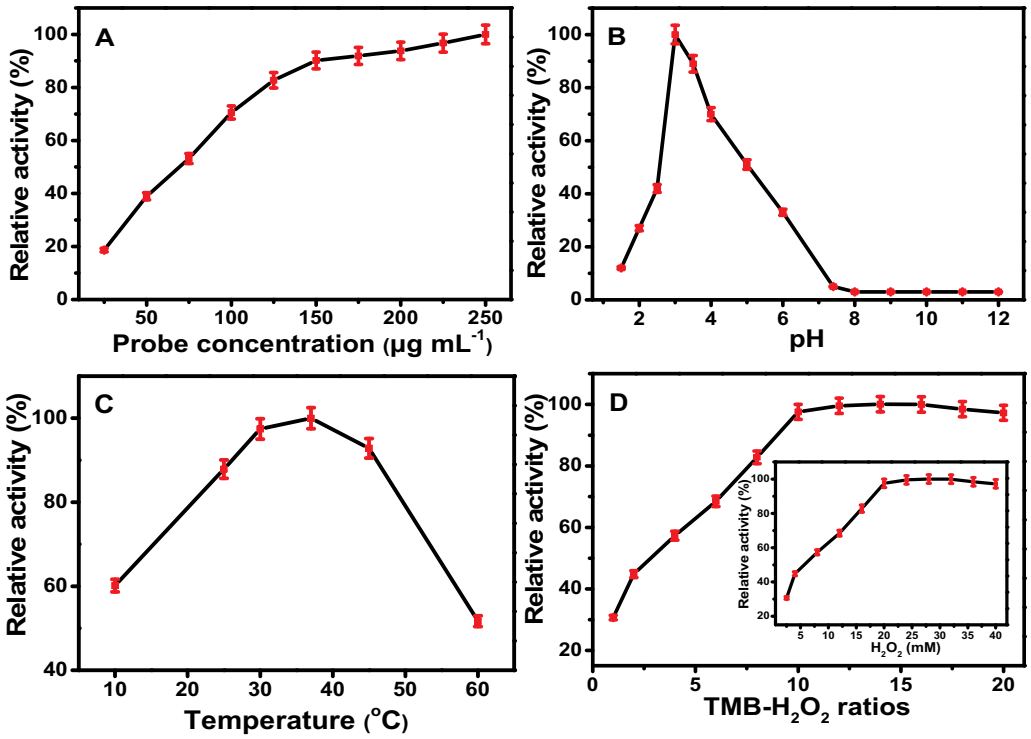

Fig. 4. Optimization of the detection conditions for the peroxidase-like catalysis of PEI-DHB NPs, including (A) PEI-DHB NPs dosage; (B) different pH values; (C) reaction temperature; (D) TMB-H_2O_2 ratios (insert: H_2O_2 concentrations-dependent catalysis of PEI-DHB NPs).

3.4. Selective responses of PEI-DHB NPs to heparin

The as-fabricated PEI-DHB NPs with peroxidase-like catalysis activities were utilized for the colorimetric assays for heparin in buffer. Relative absorbance values of the resulting catalytic TMB-H_2O_2 reactions, which is defined as $[(A_0 - A) / A_0]$ (λ_{max} = 652 nm), where A and A_0 refer to the absorbance in the presence and absence of heparin, respectively. Fig. 6 manifests the PEI-DHB NPs catalytic TMB-H_2O_2 reactions selectively inhibited by heparin in comparison with other small molecules and ions possibly coexisting in biological samples. It was discovered that the addition of heparin caused the obvious inhibition of the catalysis of PEI-DHB NPs showing the decrease in the

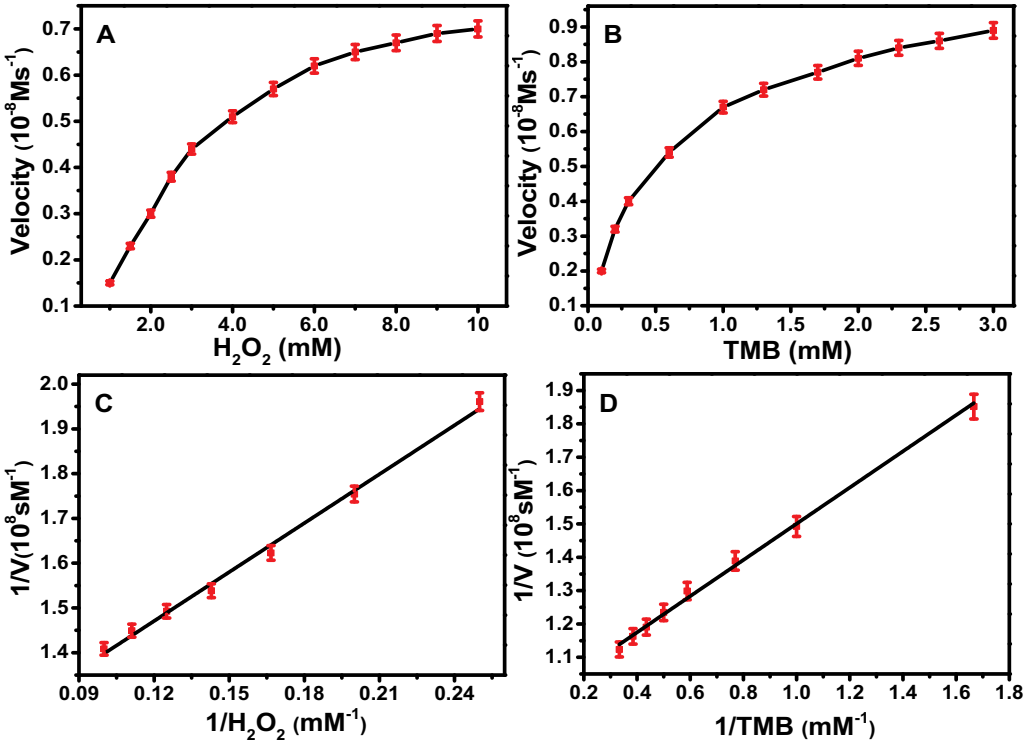

Fig. 5. Steady-state kinetic studies of PEI-DHB NPs by the colorimetric measurements using (A) 2.0 mM TMB and varying concentrations of H_2O_2; (B) 20.0 mM H_2O_2 and varying concentrations of TMB (the error bars represent the standard deviations of three repeated measurements); double reciprocal plotting for investigating the catalysis activity of PEI-DHB NPs using the fixed concentration of (C) H_2O_2; (D) TMB and varying concentrations of TMB and H_2O_2, respectively.

Table 1
Comparison of the apparent Michaelis-Menten constant (K_m) and maximum reaction rate (V_{max}) among PEI-DHB NPs and other kinds of metal-free peroxidase mimics.

Artificial enzyme	Substrates	K_m (mM)	$V_{max}(10^{-8}$ MS$^{-1})$	Ref.s
SWCNH$_S$-COOH	H_2O_2	49.80	2.07	[14]
	TMB	0.506	2.28	
$C_{60}[C(COOH)_2]_2$	H_2O_2	24.58	4.01	[41]
	TMB	0.233	3.47	
Carboxyfluorescein	H_2O_2	3.70	2.89	[16]
	TMB	0.26	2.92	
PEI-DHB NPs	H_2O_2	3.52	0.97	This work
	TMB	0.56	1.03	

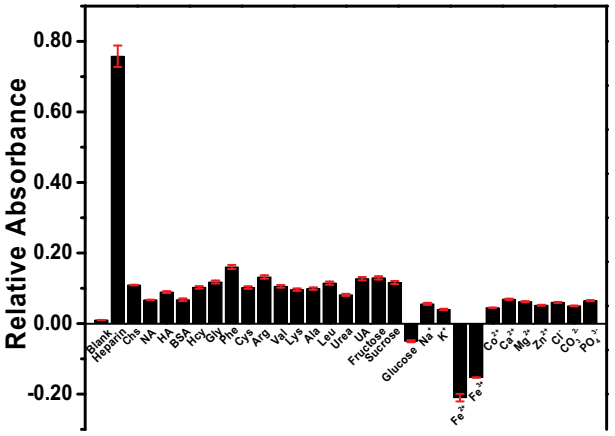

Fig. 6. Colorimetric investigations of the PEI-DHB NPs-catalyzing TMB-H_2O_2 reactions depressed by heparin (10.0 μM) in comparison with other possibly interfering substances of small molecules (1.0 mM) and ions (10 mM), including Chs, NA, HA, BSA, Hcy, Gly, Phe, Cys, Arg, Val, Lys, Ala, Leu, urea, UA, Fru, Suc, Glu, Na^+, K^+, Fe^{2+}, Fe^{3+}, Co^{2+}, Ca^{2+}, Mg^{2+}, Zn^{2+}, Cl^-, CO_3^{2-}, and PO_4^{3-} ions.

absorbance spectra of the reactant products. In contrast, negligible variations of the relative absorbance values were obtained for 29 kinds of other small molecules possibly con-existing in serum with the common levels so tested, even including the chondroitin sulfate sodium salt (Chs) and hyaluronic acid (HA) sharing the heparin-similar molecular structures. Herein, PEI in PEI-DHB NPs, as a positively-charged polyelectrolyte, can endow the nanozyme with positive charges of high density as aforementioned. These negatively-charged small molecules and ions so tested might electrostatically interact with the nanozyme,

Table 2
Comparison of the heparin analysis results among the developed colorimetric method with PEI-DHB nanozyme with other analysis techniques with different artificial enzymes.

Probes	Detection limit (μM)	Linear range (μM)	Ref.s
Cationic polymer	0.03	0.03–48.0	[33]
Polydiacetylene liposome	–	2.5–45.0	[38]
Functionalised pyrene	3.50	1.0–10.0	[42]
HPQ-TBP-I	0.022	0.0–14.0	[43]
PEI-DHB NPs	0.017	0.05–1.0	This work

which, however, is not strong enough to inhibit its catalytic activity sites. In contrast, heparin as a negatively-charged polyelectrolyte can present much stronger electrostatic adsorption with oppositely-charged PEI-DHB NPs than other small molecules (i.e., amino acids) or ions tested. As a result, heparin can conduct the stronger inhibition on peroxidase-like catalysis of PEI-DHB NPs than these possible interferents indicated. The data of control tests confirm that the colorimetric strategy with PEI-DHB NPs could exhibit the excellent selectivity in sensing heparin.

3.5. Colorimetric analysis performance for heparin with PEI-DHB NPs

The developed colorimetric analysis method with PEI-DHB NPs was applied for probing heparin with different concentrations in buffer (Fig. 7). As described in Fig. 7A, the absorption values of TMB-H_2O_2 reaction products could progressively decrease with incremental amounts of heparin. A linear relationship between the relative absorbance values versus the heparin concentrations was obtained over the linear range of 0.010–1.0 μM (Fig. 7B, insert), with the limit of detection of 2.5 nM, estimated by the 3σ rule. Moreover, a comparison of the heparin analysis results was conducted among the developed colorimetric method and the current analysis techniques documented with other artificial enzymes (Table 2). By comparison, one can see that the developed colorimetric strategy with the probes of PEI-DHB NPs can display the better or comparable analysis performances for the detection of heparin in terms of linear concentration range and detection limit.

3.6. Practical application of the PEI-DHB NPs-based colorimetric method for heparin in serum samples

In order to further explore the practical application feasibility, the developed PEI-DHB NPs-based sensing strategy was employed to evaluate heparin spiked in serum samples with different levels (Fig. 8). One can find that a linear calibration curve (R^2 = 0.9892) was obtained by

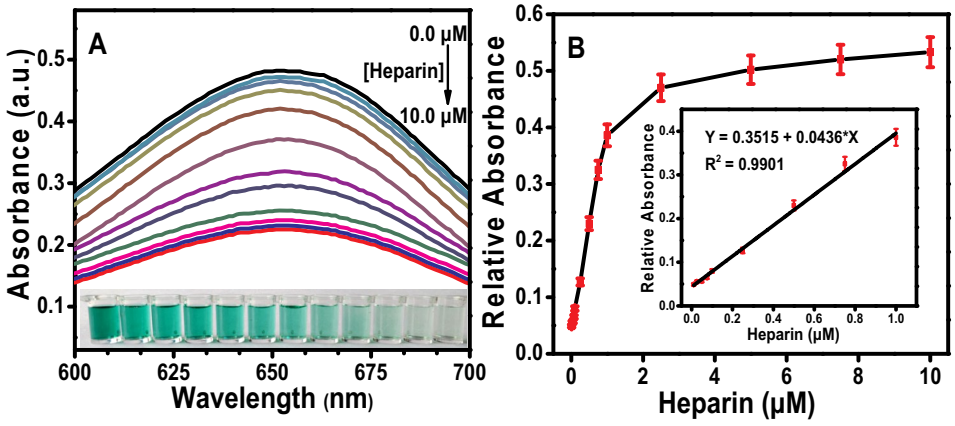

Fig. 7. (A) UV–vis absorption spectra of colorimetric responses of PEI-DHB NPs-catalyzing TMB-H_2O_2 reactions to heparin with different concentrations in buffer (0.0–10.0 μM); (B) the relationship between the relative absorbance values versus heparin concentrations.

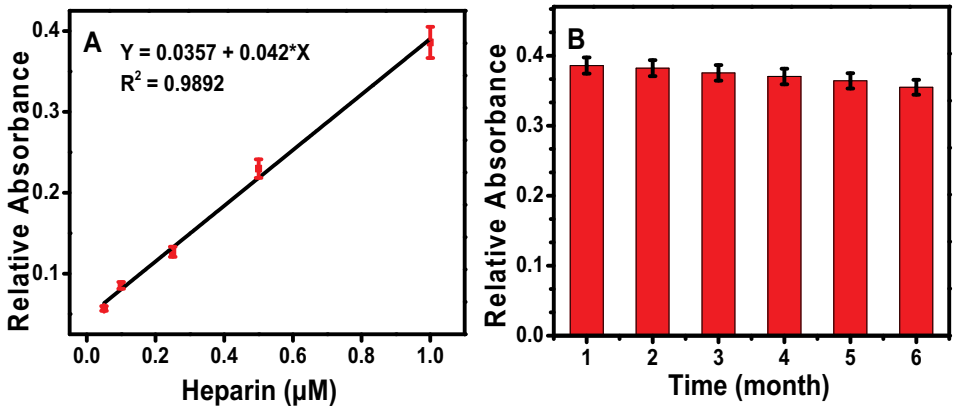

Fig. 8. The calibration curve for the relative absorbance values versus (A) heparin concentrations in serum (0.050–1.0 μM). (B) The relative absorbance values for testing heparin depending on the storage time of PEI-DHB NPs for different time intervals.

plotting the relative absorbance values versus the heparin concentrations over a linear range of 0.050–1.0 μM (Fig. 8A), of which the detection limit was determined to be 0.017 μM. Moreover, the environmental stability of PEI-DHB NPs for the colorimetric detections of heparin was investigated using PEI-DHB NPs which were stored at 4 °C over different time intervals and then taken out for the catalysis experiments (Fig. 8B). The results indicate that the colorimetric efficiencies might show no significant change over time up to six months. Therefore, the developed colorimetric analysis method may promise the practical applicability for monitoring heparin with low levels in some complicated samples like serum.

4. Conclusions

In conclusion, metal-free polymer nanozymes of PEI-DHB NPs were initially synthesized simply via the catalyst-free one-pot covalent reaction using environmentally friendly hyperbranched PEI with redox DHB in aqueous media. Compared with the current artificial enzymes especially those of inorganic metal-based artificial enzymes, the developed polymer nanozymes can feature some advantages such as low toxicity, good water solubility, cost-effectiveness, and high environmental stability over the wide H_2O_2 concentrations. Moreover, the peroxidase-like catalysis activity of the metal-free nanozymes could be specifically inhibited by heparin serving as the oppositely-charged capping agent. A facile and sensitive visualized colorimetric method has thereby been developed for the detection of heparin in serum, with the level down to 0.017 μM. Importantly, such a simple and green polymer-based synthesis route may open a new door toward the one-pot fabrication of various metal-free nanozymes to promise the extensive catalysis applications for the evaluations of a variety of targets of great importance in the biomedical analysis, food safety, environmental monitoring, and drug screening fields.

Acknowledgments

This work is supported by the National Natural Science Foundation of China (No. 21675099 and 21375075), Major Basic Research Program of Natural Science Foundation of Shandong Province (ZR2018ZC0129), and Key Research and Development Plan of Jining City (2018HMNS001), P. R. China.

References

[1] H. Wei, E.K. Wang, Nanomaterials with enzyme-like characteristics (nanozymes): next-generation artificial enzymes, Chem. Soc. Rev. 42 (2013) 6060–6093.
[2] Z.T. Yang, J. Qian, X.W. Yang, D. Jiang, X.J. Du, K. Wang, H.P. Mao, K. Wang, A facile label-free colorimetric aptasensor for acetamiprid based on the peroxidase-like activity of hemin-functionalized reduced graphene oxide, Biosens. Bioelectron. 65 (2015) 39–46.
[3] C.Q. Wang, J. Qian, K. Wang, X.W. Yang, Q. Liu, N. Hao, C.K. Wang, X.Y. Dong, X.Y. Huang, Colorimetric aptasensing of ochratoxin A using Au@Fe_3O_4 nanoparticles as signal indicator and magnetic separator, Biosens. Bioelectron. 77 (2016) 1183–1191.
[4] L.Z. Gao, J. Zhuang, L. Nie, J.B. Zhang, Y. Zhang, N. Gu, T.H. Wang, J. Feng, D.G. Yang, S. Perrett, X.Y. Yan, Intrinsic peroxidase-like activity of ferromagnetic nanoparticles, Nat. Nanotechnol. 2 (2007) 577–583.
[5] R. Bhattacharjee, S. Tanaka, S. Moriam, M.K. Masud, J.J. Lin, S.M. Alshehri, T. Ahamad, R.R. Salunkhe, N.T. Nguyen, Y. Yamauchi, M.S.A. Hossain, M.J.A. Shiddiky, Porous nanozymes: the peroxidase-mimetic activity of mesoporous iron oxide for the colorimetric and electrochemical detection of global DNA methylation, J. Mater. Chem. B 6 (2018) 4783–4791.
[6] M.N. Islam, M.K. Masud, N.T. Nguyen, V. Gopalan, H.R. Alamri, Z.A. Alothman, M.S. Al Hossain, Y. Yamauchi, A.K. Lam, M.J.A. Shiddiky, Gold-loaded nanoporous ferric oxide nanocubes for electrocatalytic detection of microRNA at attomolar level, Biosens. Bioelectron. 101 (2018) 275–281.
[7] M.N. Islam, L. Gorgannezhad, M.K. Masud, S. Tanaka, M.S.A. Hossain, Y. Yamauchi, N.T. Nguyen, M.J.A. Shiddiky, Graphene oxide-loaded iron oxide superparamagnetic nanoparticles for ultrasensitive electrocatalytic detection of microRNA, Chem. Electr. Chem. 5 (2018) 2488–2495.
[8] M.K. Masud, S. Yadav, M.N. Islam, N.T. Nguyen, C. Salomon, R. Kline, H.R. Alamri, Z.A. Alothman, Y. Yamauchi, M.S.A. Hossain, M.J.A. Shiddiky, Gold-loaded nanoporous ferric oxide nanocubes with peroxidase-mimicking activity for electrocatalytic and colorimetric detection of autoantibody, Anal. Chem. 89 (2017) 11005–11013.
[9] J. Qian, X.W. Yang, L. Jiang, C.D. Zhu, H.P. Mao, K. Wang, Facile preparation of Fe_3O_4 nanospheres/reduced graphene oxide nanocomposites with high peroxidase-like activity for sensitive and selective colorimetric detection of acetylcholine, Sensors Actuators B Chem. 201 (2014) 160–166.
[10] H. Wang, S. Li, Y.M. Si, N. Zhang, Z.Z. Sun, H. Wu, Y.H. Lin, Platinum nanocatalysts loaded on graphene oxide-dispersed carbon nanotubes with greatly enhanced peroxidase-like catalysis and electrocatalysis activities, Nanoscale 6 (2014) 8107–8116.
[11] L.Y. Zhang, S. Li, M.M. Dong, Y. Jiang, R. Li, S. Zhang, X.X. Lv, L.J. Chen, H. Wang, Reconstituting redox active centers of heme-containing proteins with biomineralized gold toward peroxidase mimics with strong intrinsic catalysis and electrocatalysis for H_2O_2 detection, Biosens. Bioelectron. 87 (2017) 1036–1043.
[12] Z. Zhou, N. Hao, Y. Zhang, R. Hua, J. Qian, Q. Liu, H.N. Li, W.H. Zhu, K. Wang, A novel universal colorimetric sensor for simultaneous dual target detection through DNA-directed self-assembly of graphene oxide and magnetic separation, Chem. Commun. 53 (2017) 7096–7099.
[13] W.B. Shi, Q.L. Wang, Y.J. Long, Z.L. Cheng, S.H. Chen, H.Z. Zheng, Y.M. Huang, Carbon nanodots as peroxidase mimetics and their applications to glucose detection, Chem. Commun. 47 (2011) 6695–6697.
[14] A.X. Zheng, Z.X. Cong, J.R. Wang, J. Li, H.H. Yang, G.N. Chen, Highly-efficient peroxidase-like catalytic activity of graphene dots for biosensing, Biosens. Bioelectron. 49 (2013) 519–524.
[15] S.Y. Zhu, X.E. Zhao, J.M. You, G.B. Xu, H. Wang, Carboxylic-group-functionalized single-walled carbon nanohorns as peroxidase mimetics and their application to glucose detection, Analyst 140 (2015) 6398–6403.
[16] Q. Hu, L. Li, G.Z. Sun, D.L. Li, J.M. Kong, W. Huang, X.J. Zhang, 5-Carboxyfluorescein: intrinsic peroxidase-like catalytic activity and its application in the biomimetic synthesis of polyaniline nanoplatelets, J. Mater. Chem. B 5 (2017) 5937–5941.
[17] X. Huang, Y. Liu, K. Liang, Y. Tang, J.Q. Liu, Construction of the active site of glutathione peroxidase on polymer-based nanoparticles, Biomacromolecules 9 (2008) 1467–1473.
[18] T. Tay, E. Köse, R. Keçili, R. Say, Design and preparation of nano-lignin peroxidase (NanoLiP) by protein block copolymerization approach, Polymers 8 (2016) 223–232.
[19] S. Taranejoo, J. Liu, P. Verma, K. Hourigan, A review of the developments of

characteristics of PEI derivatives for gene delivery applications, J. Appl. Polym. Sci. 132 (2015) 42096–42103.
[20] J.S. Liu, G.N. Liu, W.X. Liu, Y.R. Wang, Turn-on fluorescence sensor for the detection of heparin based on rhodamine B-modified polyethyleneimine-graphene oxide complex, Biosens. Bioelectron. 64 (2015) 300–305.
[21] H. Eskandarloo, M. Godec, M. Arshadi, O.I. Padilla-Zakour, A. Abbaspourrad, Multiporous quaternized chitosan/polystyrene microbeads for scalable, efficient heparin recovery, Chem. Eng. J. 348 (2018) 399–408.
[22] D.L. Rabenstein, Heparin and heparan sulfate: structure and function, Nat. Prod. Rep. 19 (2002) 312–331.
[23] I. Capila, R.J. Linhardt, Heparin-protein interactions, Angew. Chem. Int. Ed. 41 (2002) 390–412.
[24] B.H. Chong, J.H. Chong, Heparin-induced thrombocytopenia, N. Engl. J. Med. 373 (2015) 252–261.
[25] J.F.K. Limtiaco, C.J. Jones, C.K. Larive, Characterization of heparin impurities with HPLC-NMR using weak anion exchange chromatography, Anal. Chem. 81 (2009) 10116–10123.
[26] T. Beyer, B. Diehl, G. Randel, E. Humpfer, H. Schäfer, M. Spraul, C. Schollmayer, U. Holzgrabe, Quality assessment of unfractionated heparin using ^{1}H nuclear magnetic resonance spectroscopy, J. Pharm. Biomed. Anal. 48 (2008) 13–19.
[27] R.P. Patel, C. Narkowicz, J.P. Hutchinson, E.F. Hilder, G.A. Jacobson, A simple capillary electrophoresis method for the rapid separation and determination of intact low molecular weight and unfractionated heparins, J. Pharm. Biomed. Anal. 46 (2008) 30–35.
[28] J. Langmaier, E. Samcová, Z. Samec, Potentiometric sensor for heparin polyion: transient behavior and response mechanism, Anal. Chem. 79 (2007) 2892–2900.
[29] S.L. Dong, X.J. Liu, Q.Q. Zhang, W.F. Zhao, C.H. Zong, A.Y. Liang, H.W. Gai, Sensing active heparin by counting aggregated quantum dots at single-particle level, ACS Sens. 2 (2017) 80–86.
[30] P. Thirupathi, J.Y. Park, L.N. Neupane, M.Y.L.N. Kishore, K.H. Lee, Pyrene excimer-based peptidyl chemosensors for the sensitive detection of low levels of heparin in 100% aqueous solutions and serum samples, ACS Appl. Mater. Interfaces 7 (2015) 14243–14253.
[31] C.D. Sommers, D.A. Keire, Detection of possible economically motivated adulterants in heparin sodium and low molecular weight heparins with a colorimetric microplate based assay, Anal. Chem. 83 (2011) 7102–7108.
[32] T. Bříza, Z. Kejík, I. Císařová, J. Králová, P. Martásek, V. Král, Optical sensing of sulfate by polymethinium salt receptors: colorimetric sensor for heparin, Chem. Commun. 16 (2008) 1901–1903.
[33] K.Y. Pu, B. Liu, A multicolor cationic conjugated polymer for naked-eye detection and quantification of heparin, Macromolecules 41 (2008) 6636–6640.
[34] J.G. You, Y.W. Liu, C.Y. Lu, W.L. Tseng, C.J. Yu, Colorimetric assay of heparin in plasma based on the inhibition of oxidase-like activity of citrate-capped platinum nanoparticles, Biosens. Bioelectron. 92 (2017) 442–448.
[35] R. Cao, B.X. Li, A simple and sensitive method for visual detection of heparin using positively-charged gold nanoparticles as colorimetric probes, Chem. Commun. 47 (2011) 2865–2867.
[36] S. Miller, Naked-eye colorimetric analysis of heparin and its derivatives, Anal. Chem. 82 (2010) 2865–2867.
[37] X.L. Fu, L.X. Chen, J.H. Li, M. Lin, H.Y. You, W.H. Wang, Label-free colorimetric sensor for ultrasensitive detection of heparin based on color quenching of gold nanorods by graphene oxide, Biosens. Bioelectron. 34 (2012) 227–231.
[38] Y.S. Cho, K.H. Ahn, Molecular interactions between charged macromolecules: colorimetric detection and quantification of heparin with a polydiacetylene liposome, J. Mater. Chem. B 1 (2013) 1182–1189.
[39] L. Liu, Y. Shi, Y.F. Yang, M.L. Li, Y.J. Long, Y.M. Huang, H.Z. Zheng, Fluorescein as an artificial enzyme to mimic peroxidase, Chem. Commun. 52 (2016) 13912–13915.
[40] J.J. Virgen-Ortiz, J.C.S. dos Santos, A.B. Murcia, O. Barbosa, R.C. Rodrigues, R.F. Lafuente, Polyethylenimine: a very useful ionic polymer in the design of immobilized enzyme biocatalysts, J. Mater. Chem. B 36 (2017) 7461–7490.
[41] R.M. Li, M.M. Zhen, M.R. Guan, D.Q. Chen, G.Q. Zhang, J.C. Ge, P. Gong, C.R. Wang, C.Y. Shu, A novel glucose colorimetric sensor based on intrinsic peroxidase-like activity of C_{60}-carboxyfullerenes, Biosens. Bioelectron. 47 (2013) 502–507.
[42] C.W. Chan, D.K. Smith, Pyrene-based heparin sensors in competitive aqueous media - the role of self-assembled multivalency (SAMul), Chem. Commun. 52 (2016) 3785–3788.
[43] S. Li, M. Gao, S. Wang, R. Hu, Z. Zhao, A. Qin, B.Z. Tang, Light up detection of heparin based on aggregation-induced emission and synergistic counter ion displacement, Chem. Commun. 53 (2017) 4795–4798.
[44] L. Ma, N.N. Sun, Y.Y. Meng, C.H. Tu, X.Q. Cao, Y.C. Wei, L.Q. Chu, A.P. Diao, Harnessing the affinity of magnetic nanoparticles toward dye-labeled DNA and developing it as an universal aptasensor revealed by lipopolysaccharide detection, Anal. Chim. Acta 1036 (2018) 107–114.